Indian Journal of Pure & Applied Physics
Vol. 62, July 2024, pp. 593-606
DOI: 10.56042/ijpap.v62i7.7784

# The Influence of Isoleucine on Structural, Optical and Electrical Properties of Lithium Dihydrogen Phosphate Crystal

H K Ladani[a*], K V Vadhel[b], H Bhuva[a], D B Mankad[a], V J Pandya[a], Radhika Rathod[a] & H O Jethva[a]

[a]Department of Physics, Saurashtra University, Rajkot, Gujarat 360 005, India
[b]Department of Physics, Indrashil University, Rajpur (Kadi), Gujarat, 382 740, India

*Received 4 January 2024; accepted 1 May 2024*

The present investigation systematically explores the impact of isoleucine doping on the structural, optical, and electrical properties of lithium dihydrogen phosphate (LDP) crystals. Pure and isoleucine-doped LDP crystals with various dopant concentrations (0.3, 0.6, and 0.9 wt%) have been synthesized using the slow solvent evaporation technique. Structural analysis utilizing X-ray diffraction revealed a reduction in crystallite size and a reduction in the compressive and tensile strains induced by isoleucine integration. Optical examinations showcased a gradual reduction in the bandgap energy alongside an increase in the Urbach energy with escalating dopant concentration, indicating increase in structural disorder. Moreover, the extinction coefficient, optical conductivity, and refractive index show an upward trajectory with doping, while optical density exhibits an inverse correlation. Electrical characterization that include dielectric and impedance spectroscopic methods showed a decline in DC conductivity and a rise in grain resistance, attributable to diminished charge carrier mobility and density. The power law exponent indicated ideal long range path ways and diffusion limited hopping mechanism. The relaxation kinetics exhibited deviation from ideal Debye behavior, with the stretch exponent parameter signifying an improvement in relaxation dynamics at higher doping levels. The complex impedance and modulus plot analysis showed the dominancy of grain relaxation mechanism within the range of frequency studied. In summary, this exhaustive investigation shows the intricate interplay between isoleucine doping and the diverse properties of LDP crystals, offering valuable insights for potential applications.

**Keywords:** LDP; Powder XRD; Optical parameters; Complex impedance; Modulus plots

## 1 Introduction

In the growth and characterization of single crystal of lithium dihydrogen phosphate, having formula $LiH_2PO_4$ and abbreviated as LDP has attracted a great deal of attention of the researchers due to high electrical conductivity[1,2], piezoelectric and elastic properties[3], anomalies in dielectric constant and electrical conductivity[2], promising material for a wide variety of electrochemical devices[4]. The structural, optical, and electrical spectroscopic characteristics have been extensively investigated by numerous researchers in the field. These studies have contributed significantly to our understanding of the material properties and their implications for various applications[5-9]. According to literature[10], two types of hydrogen bonds were reported in LDP and they connect $PO_4$ tetrahedra, building a three dimensional framework. As LDP is protonic conductor, the conduction mechanism in LDP is due to the motion of hydrogen within this three dimensional framework of its structure. In the literature, an increase in electrical conductivity of LDP on subsequent heating is reported, which is due to the improved mobility of hydrogen ions on heating[2]. The reported protonic conductivity of solid LDP at room temperature is of the order of $10^{-5}$ to $10^{-4}$ S/cm, which is relatively higher compared to that of solid $NaH_2PO_4$, $KH_2PO_4$ and $CsH_2PO_4$[4]. In the literature, growth of pure LDP crystals have been reported by two methods, *i.e*., from aqueous solution containing excess of $H_3PO_4$ content using solvent evaporation[2,3,11] and temperature lowering method[12,13]. No reports are available in the literature on the growth and effect of amino acid doping on the various properties of LDP crystals. It has been reported that the doping of amino acids having hydrogen bonded side chain may lead to either increase or decrease in the conductivity of amino acids doped ADP and KDP crystals. As the conduction in LDP is protonic and isoleucine, having condensed formula ($C_6H_{13}NO_2$) and expanded molecular formula $CH_3CH_2(CH_3)CH(NH_2)CHCOOH$, itself contains a hydrogen bonded long side chain

*Corresponding author: (E-mail: happyladani18@gmail.com)

$CH_3CH_2(CH_3)CH$, it will be interesting to study the effect of doping of isoleucine on the various properties of LDP. The consequences of doping depend of course on, dopant concentration as well as on the related factors such as strain in the crystal lattice of host material, peak (generally most intense peak) shift and variation in peak intensity and FWHM of host material, the presence of grain and/or grain boundaries and the crystallite alignment[14,15].

In the present study, the authors have undertaken a comprehensive investigation of the structural and linear optical properties, including the Tauc plot, Urbach energy, extinction coefficient, skin depth, refractive index, optical conductivity, optical density, and electrical susceptibility, as well as dielectric, impedance, and modulus spectroscopic properties of both pure and 0.3wt%, 0.6wt% and 0.9wt% doped Lithium Dihydrogen Phosphate crystals. This study marks the first exploration of these properties, offering novel insights into the behavior of these crystals under various conditions.

## 2 Experimental

### 2.1 Sample Preparation

Lithium dihydrogen phosphate (LDP) (99% purity) and isoleucine (98%) were procured from Sigma Aldrich. The pure crystals of LDP and different weight % (0.3wt%, 0.6wt% and 0.9 wt%) isoleucine doped LDP were prepared by using slow solvent evaporation technique at room temperature. Known amount of LDP was dissolved in 400 ml distilled water and stirred well to prepare homogeneous saturate solution of pure LDP. This solution was divided equally in to four beakers. In three beakers, 0.3g, 0.6g and 0.9g isoleucine was added and again stirred well to prepare homogeneous solution of isoleucine added LDP. All the solutions were filtered and covered the beakers with filter paper having four pin holes for the controlled evaporation and placed in a dust and disturbance free place in the laboratory. After the complete evaporation, good quality and transparent crystals of pure and isoleucine doped LDP, having flower shaped morphology were harvested for different experimental studies. Fig. 1 shows the photographs of the pure and isoleucine doped LDP crystals.

### 2.2 Characterization

Structural behavior of pure and isoleucine doped LDP crystals were examined by means of XRD analysis. XRD patterns were recorded on PANaylitcal X'pert pro set up by using Cu $K_\alpha$ radiation within 2θ range $10^o$ to $80^o$ in steps of $0.02^o$ $sec^{-1}$. In order to deduce various optical parameters of pure and isoleucine doped LDP crystals, the UV-Vis data were recorded on Shimadzu UV-1700 Phamaspec by adopting dissolution method having HPLC grade water as internal standard. The maximum transmission and absorbance (in %) was measured by injecting the samples directly into UV spectrometer. Obtained UV chromatogram was recorded by Shimadzu UV prob 2.6 software. The dielectric behavior of pure and isoleucine doped LDP crystals was measured by a Precision LCR meter Agilent 4284A instrument in the frequency range of 100 Hz to 1 MHz at room temperature, by placing each pelletized sample turn by turn between sample holder.

## 3 Results and Discussion

### 3.1 Powder XRD study

The influence of different wt% isoleucine doping on the crystal structure of pure LDP crystal was examined through powder XRD analysis. The resultant patterns of pure and isoleucine doped LDP crystals are shown in the Fig. 2. The unit cell parameters are tabulated in the Table 1.

The XRD peaks at 2θ values of $22.5^o$, $35.2^o$, $27.4^o$, $33.7^o$, $31.5^o$, $17.4^o$, $25.9^o$ and $32^o$ correspond to the planes of (111), (022), (120), (211), (201), (011), (002) and (112), respectively. The lattice parameters reported in the literature[16,17] were used as the starting lattice parameters. In the present case, the obtained lattice parameters are found close to the reported

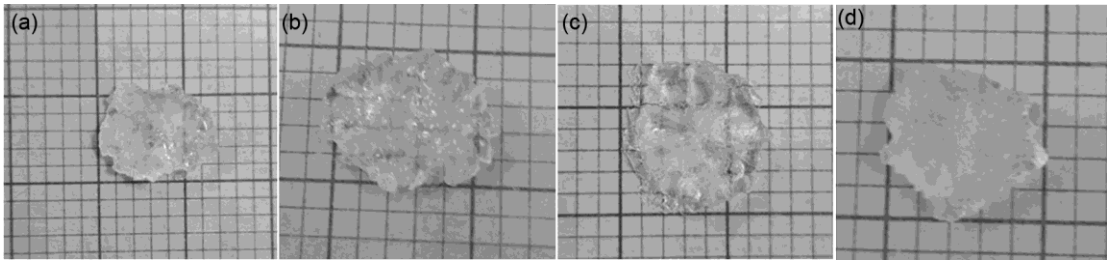


Fig. 1 — Grown crystals of (a) Pure LDP (b) 0.3Wt% (c) 0.6Wt% and (d) 0.9Wt% isoleucine doped LDP

Table 1 — Unit cell parameters

| Sample name | a (Å) | b (Å) | c (Å) | Unit cell volume (Å$^3$) |
|---|---|---|---|---|
| Pure LDP | 6.2348 | 7.6295 | 6.8658 | 326.60 |
| 0.3 Wt% isoleucine doped LDP | 6.2394 | 7.6397 | 6.8719 | 327.56 |
| 0.6 Wt% isoleucine doped LDP | 6.2369 | 7.6341 | 6.8691 | 327.06 |
| 0.9 Wt% isoleucine doped LDP | 6.2295 | 7.6201 | 6.8561 | 325.45 |

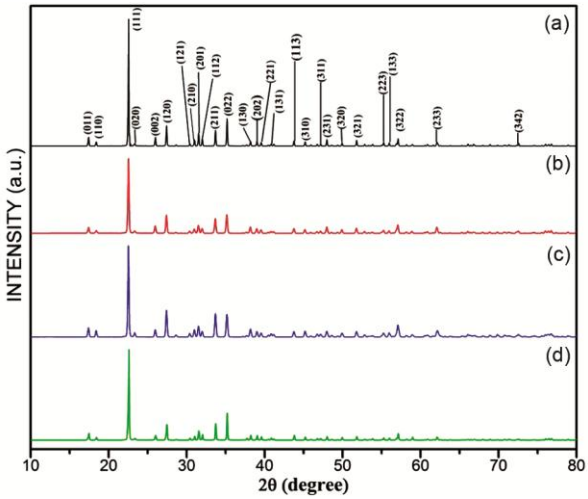


Fig. 2 — Powder XRD patterns of (a) Pure LDP (b) 0.3 wt% (c) 0.6 wt% and (d) 0.9 wt% isoleucine doped LDP crystals

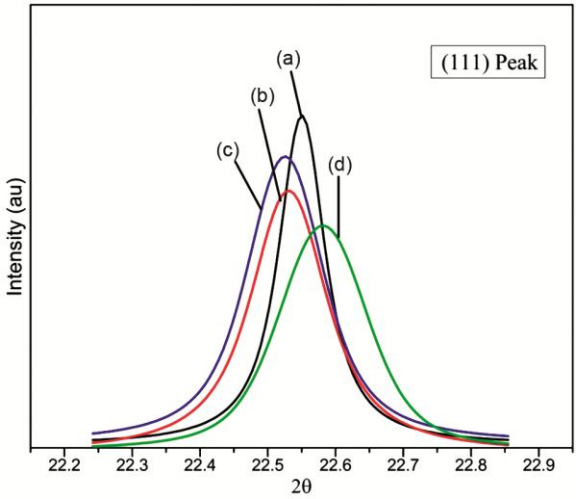


Fig. 3 — Expanded scale image of peak (111) of (a) Pure LDP (b) 0.3 wt% (c) 0.6 wt% and (d) 0.9 wt% isoleucine doped LDP crystals

values. All the peaks indicate that pure as well as isoleucine doped LDP crystals are orthorhombic in structure. The sharp diffraction peaks indicate good crystallinity of the grown crystals. The most intense peak (111) of pure LDP was chosen to study the effect of doping of isoleucine and change in its weight %.

The expanded scale image of (111) peak is shown in the Fig. 3.

From the Fig. 3, it is observed that the doped LDP crystals show reduced intensity, shifting of peak and increased FWHM. The reduced intensity of diffraction peak indicate reduced crystallinity of isoleucine doped LDP crystals, while the shifting and broadening of the peak indicates the presence of uniform strain and non-uniform strain, respectively[18]. The peaks in Fig. 3 show a shift in peak position with increase in dopant concentrations compared to pure LDP crystals. The peaks for the samples with 0.3wt% and 0.6wt% isoleucine doped LDP crystals, indicating expansion in the lattice, while for 0.9wt% isoleucine doped LDP crystals shift to higher values of diffraction angle, indicating shrinkage in the lattice[19]. The peaks are wider for the isoleucine doped LDP crystals, which indicates non-uniformity of strain. The types of strain are evaluated by applying the Williamson-Hall method to the powder X-ray diffraction data.

The X-ray diffraction patterns are influenced by the size of crystallite as well as by the lattice strain and lattice defects. Williamson-Hall method is a simplified method of analysis that clearly differentiates the size and strain induced deformation peak considering the broadening of the peak width as a function of diffraction angle 2 theta. By W-H method, the separation of size and strain effects is possible according to the equation[20]:

$$\beta\cos\theta = (k\lambda/D) + 4\varepsilon\sin\theta, \quad \ldots(1)$$

where, β represents the full width at half maximum (FWHM in radian) of a radiant peak, $D$ and ε correspond to the value of the crystallite size and micro strain, respectively, $k$ is the shape factor, $\lambda$ is the X-ray wavelength (1.54056 Å) and $\theta$ is the diffraction angle of Bragg. A plot between βcosθ and 4sinθ produces a straight line that facilitates the extraction of lattice strain (ε) from the slope of the straight line and crystallite size from the intercept. The result of the W-H analysis is tabulated in the Table 2.

It is observed from the Table 2 that crystallite size is decreased with isoleucine doping. It may be due to

Table 2 — Crystallite size and strain values of isoleucine doped LDP crystals

| Sample name | W-H method | |
|---|---|---|
| | D (nm) | $\varepsilon \times 10^{-5}$ |
| Pure LDP | 64.49 | –1.90 |
| 0.3 wt% isoleucine doped LDP | 57.30 | –24.4 |
| 0.6 wt% isoleucine doped LDP | 48.82 | –4.34 |
| 0.9 wt% isoleucine doped LDP | 36.77 | 75.00 |

the fact that the presence of isoleucine molecule requires a less reaction time to form the end product and can decrease the growth of the crystalline dimension in the nucleation centers. From the values of strain listed in the Table 2, it is observed that pure and 0.3wt% and 0.6wt% isoleucine doped LDP crystals possess negative value of slope and the value of which is increased for the 0.3wt% and 0.6wt% isoleucine doped LDP crystals. It indicates that pure and 0.3wt% and 0.6wt% isoleucine doped LDP crystals are under the influence of compressive strain, the value of which is increased for 0.3wt% and 0.6wt% isoleucine doped LDP crystals. For the 0.9wt% isoleucine doping in pure LDP, micro strain shows large positive value. This indicates that the presence of isoleucine in the highest wt%, *i.e.*, 0.9wt% creates the tensile strain in the crystal lattice of pure LDP[21-23]. The presence of both, *i.e.*, compressive and tensile strain in the isoleucine doped LDP crystals is reflected in terms of deterioration in crystallite size with isoleucine doping. Note that the values of lattice constants of 0.9wt% isoleucine doped LDP crystal system and pure as well as 0.3wt% and 0.6wt% isoleucine doped LDP crystal systems are found to be inconsistent regarding the types of strain. It indicates the non-uniform distribution of strain, which results into irregular growth and non-uniform adsorption of the impurity on the growing face. It can also be attribute to the distortion of the crystal lattice up to certain extent due to the presence of isoleucine rather than disturbing the entire lattice structure of pure LDP crystal.

### 3.2 Linear Optical Analysis

#### *3.2.1 Measurements of Optical Bandgap*

In order to evaluate the bandgap values of pure and isoleucine doped LDP crystals, Tauc's equation, which signifies a relation between absorption coefficient (α) and bandgap ($E_g$), is carried out. Tauc's equation can be expressed as[24]:

$$\alpha h\nu = A(h\nu - E_g)^n, \quad \ldots(2)$$

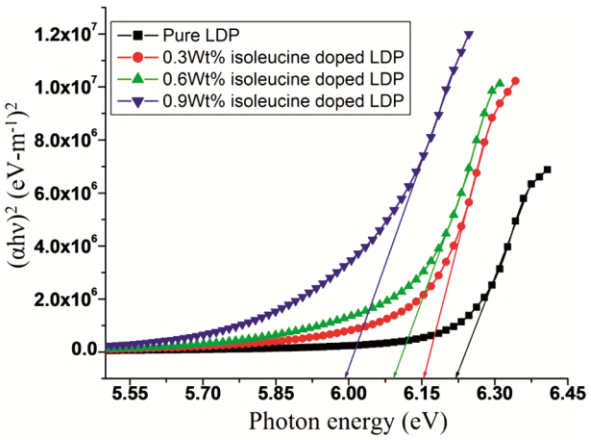


Fig. 4 — Tauc's plot

where, *h* is Planck constant, *v* is the frequency of incident photons, *A* is constant of the material and *n* is the optical transition number, which takes different values corresponds to different transitions[25].

For the estimation of the direct optical bandgap of the grown crystals, $(\alpha h\nu)^2$ is plotted against photon energy (hν), as shown in the Fig. 4.

The extrapolation of the linear portion of the plot, as shown in the Fig. 4, gives the value of $E_g$, which are 6.22 eV, 6.15 eV, 6.02 eV and 5.99 eV for pure LDP, 0.3wt%, 0.6wt% and 0.9wt% isoleucine doped LDP crystals, respectively. The determined bandgap of isoleucine doped LDP crystals is low compared to pure LDP, which may be attributed to the deterioration of crystalline phase of pure LDP crystal. The narrowing of bandgap leading to a red shift of the optical absorption may be accused by means of charge transfer process between the ions $NH_3^+$, $COO^-$, $Li^+$ and $H_2PO_4^-$. Further, due to the presence of isoleucine, the formation of recombination centre may also be responsible for the reduction in bandgap value. Such effect of recombination and due to which reduction in the bandgap value is observed for $Sr^{+2}$ doped ADP crystals[26].

#### *3.2.2 Determination of Optical Parameters*

The various valuable optical parameters for pure and isoleucine doped LDP crystals are evaluated by using the various theoretical formulae given in the literature[27].

#### *3.2.3 Urbach Energy*

The effect of isoleucine doping in different wt% into the crystal lattice of pure LDP shows the formation of band tailing in the bandgap called Urbach tail and can be predicted by obeying the Urbach rule[28]:

$$\alpha = \alpha_o exp(hv/E_e), \quad \ldots(3)$$

where, $\alpha_o$ is a constant and $E_e$ is the Urbach energy, which characterize the slope of the exponential edge and measures the disorder in the structure of the material[29]. By plotting ln(α) against the incident photon energy (hν), as shown in the Fig. 5, the Urbach energy can be determined from the reciprocal slope of the linear portion.

In the Fig. 4, a straight line is fitted within energy range 6.12 to 6.36 eV for pure LDP crystal, 5.96 to 6.27 eV for 0.3wt% isoleucine doped LDP crystal, 6.90 to 6.25 eV for 0.6wt% isoleucine doped LDP crystal and 5.38 to 6.16 eV for 0.9wt% isoleucine doped LDP crystal. The reciprocal of the slope of the fitted lines for all the crystals gives the value of Urbach energy ($E_e$) for all the crystals. The obtained values of Urbach energy are 0.192 eV, 0.235 eV, 0.215 eV and 0.370 eV for pure LDP crystal, 0.3wt%, 0.6wt% and 0.9wt% isoleucine doped LDP crystals, respectively. The Urbach energy is observed to increase for isoleucine doped LDP crystals, which reveals that the doping of isoleucine decreases the crystallinity of the pure LDP crystals. Further, if the Urbach energy is compared with optical bandgap energy, it is observed that Urbach energy increases from 0.192 to 0.370 eV and optical bandgap energy decreases from 6.22 to 5.99 eV with increase in doping wt% of isoleucine. These indicate the increase of structural disorder and defects in the isoleucine doped LDP crystals, which is reflected in terms of compressive and tensile strain in the isoleucine doped LDP crystals as discussed in the powder XRD analysis. It is also observed that the values of the bandgap ($E_g$) and Urbach energy ($E_e$) follows opposite trend, *i.e.*, with increasing doping concentration of isoleucine, bandgap decreases and Urbach energy increases. The change in Urbach energy with doping concentration of isoleucine indicates that the width of localized states in the bandgap depends on the composition and this could be responsible for the variation of the bandgap with doping concentration of isoleucine.

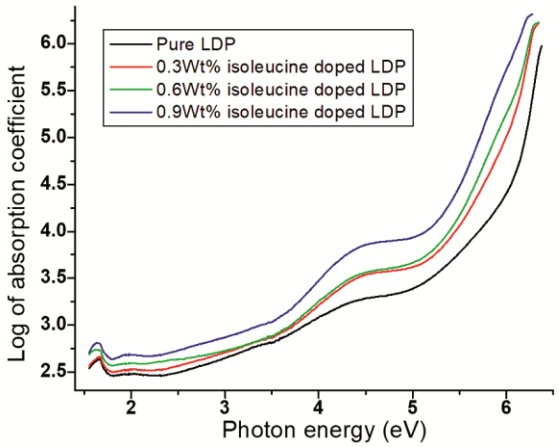


Fig. 5 — A plot of photon energy versus ln(α)

#### *3.2.4 Extinction Coefficient*

Extinction coefficient (k) of pure and isoleucine doped LDP crystals are calculated by using the relation[29]:

$$k = \alpha\lambda/4\pi, \quad \ldots(4)$$

The variation of extinction coefficient (K) with photon wavelength is shown in the Fig. 6.

The obtained extinction coefficient exhibits very low and saturate value within medium wavelength uv region (280 to 315 nm), large wavelength uv region (315 to 400 nm) and visible region (400 to 700 nm), which indicates very low absorption and hence free passage of electromagnetic radiation in that wavelength region, while below 280 nm wavelength region indicates greater degrees of opacity. It is also observed that the highest value of extinction coefficient is obtained for the 0.9wt% isoleucine doped LDP crystal, which may be due to the variation of absorption of light in the isoleucine doped LDP crystals, which is almost consistent in the higher wavelength region.

The scattering process inside pure and isoleucine doped LDP crystals was determined by using the relation[29]:

$$\delta = \lambda/2\pi k, \quad \ldots(5)$$

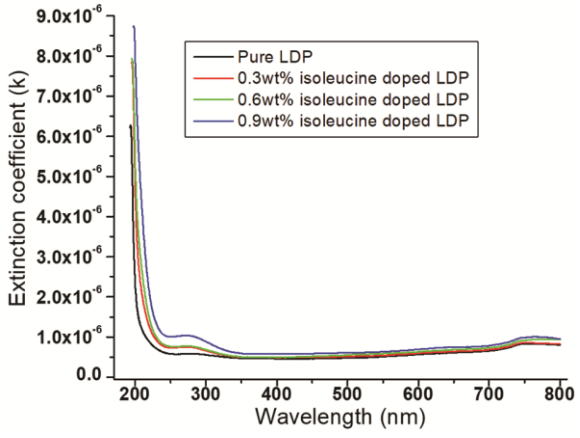


Fig. 6 — A plot of photon wavelength versus extinction coefficient (k)

where, δ is called scattering penetration depth, *i.e.*, skin depth, which is an indication of amount of penetration of electromagnetic radiation into a material.

Figure 7 shows the variation of skin depth with respect to photon energy for pure and isoleucine doped LDP crystals. The skin depth variation shows same nature for pure as well as isoleucine doped LDP crystals, *i.e.*, increases slightly in the lower photo energy region with small peaks and then decreases as the photon energy increases. The magnitude of skin depth decreases with increase in doping concentration of isoleucine in LDP crystal. This result is in accordance with the extinction coefficient and shows reduction in transmission of isoleucine doped LDP crystals. From the Fig. 7, it is observed that the skin depth is found to decrease as the value of photon energy increases up to 6.37 eV for pure LDP and up to 6.198 eV for 0.9wt% isoleucine doped LDP crystal and after that it begins to be nearly zero. The corresponding wavelength at which skin depth possesses zero value is known as cut-off wavelength. The cut-off wavelength is found to increase for isoleucine doped LDP crystals.

#### *3.2.5 Refractive Index*

The refractive index of pure and isoleucine doped LDP crystals are obtained using the relation, given in the literature[30].

Figure 8 shows the variation of refractive index with respect to wavelength for pure and isoleucine doped LDP crystals. It is observed from the Fig. 8, that the refractive index for all the grown crystals decreases as wavelength increases. This behavior can be attributed to the decrease of absorption coefficient with wavelength and hence, indicates the normal dispersion behavior of the grown crystals. Further, the curves do not show indirect proportanility of refractive index with wavelength. This behavior indicates less probability of light energy dispersion at the different interstitial layers of the crystal lattice. It is also observed from the Fig. 8 that, the magnitude of refractive index for isoleucine doped crystals increases progressively on increasing the doping concentration. The increasing behavior refractive index with doping concentration of isoleucine might be due to the structural rearrangement or some structural changes in the isoleucine doped LDP crystals. Though, the structural rearrangement or structural changes might be small enough and hence, can not disturb the entire lattice structure of pure LDP crystal.

#### 3.2.6 Optical Conductivity

The optical conductivity of pure and isoleucine doped LDP crystals is calculated by using the absorption coefficient (α) and refractive index (n) values according to relation[31]:

$$\sigma_{opt} = \alpha nc/4\pi. \qquad \ldots(6)$$

Figure 9 shows the optical conductivity against the photon energy. It is observed from the plot of Fig. 9 that, the optical conductivity increases for all the crystals with increase in photon energy, which are in consistent with the result of corresponding higher values of refractive index (n) for lower wavelength. It is noticeable that isoleucine doped LDP crystals show higher optical conductivity value than pure LDP crystal with shifting of plateau towards lower photon energy. This is in agreement with the reduced value of energy bandgap of isoleucine doped LDP crystals, as calculated from Tauc's plot. The increase in optical

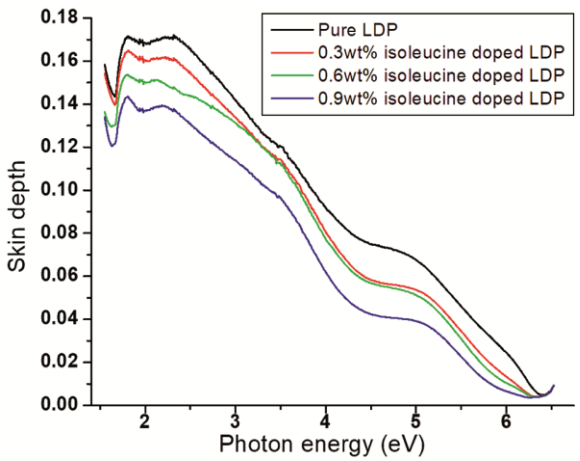


Fig. 7 — A plot of photon energy versus skin depth

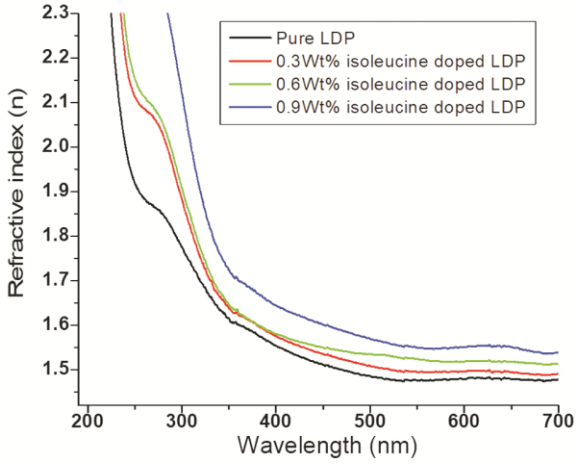


Fig. 8 — A plot of photon wavelength versus refractive index

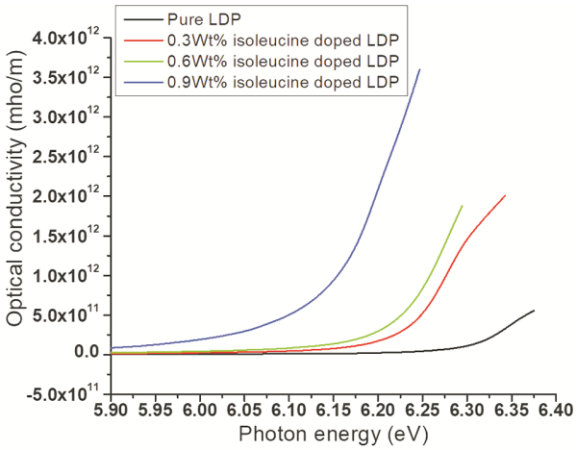


Fig. 9 — A plot of photon energy versus optical conductivity

conductivity can be attributed to the strong excitation of the electrons by photon energy[32]. The high value of optical conductivity confirms the high photo-tunable behavior of the crystals[33].

#### *3.2.7 Electrical Susceptibility*

A dimensionless parameter that determines the degree of polarization of a sample in response to the electric field applied is called electric susceptibility ($\chi_c$). Higher the value of $\chi_c$, greater is the capacity of a material to be polarized in reaction to an applied electric field. The value of ($\chi_c$) is deduced for the pure as well as isoleucine doped LDP crystals based on refractive index (n) and extinction coefficient (k) as follows[34]:

$$\chi_c = n^2 - k^2 - \varepsilon_o/4\pi, \quad \ldots(7)$$

Figure 10 shows the curves of $\chi_c$ against λ for pure as well as isoleucine doped LDP crystals. The plot of susceptibility versus wavelength shows a similar behavior as refractive index parameter n. The isoleucine doped LDP crystals show very high value of susceptibility compared to pure LDP crystal, which reveals a significant response of isoleucine doped LDP crystals to be polarized in response to the applied electric field and hence, minimizing total electric field inside the isoleucine doped LDP crystals.

#### *3.2.8 Optical Density*

A parameter that describes the refraction of electromagnetic radiation inside a material is called optical density (OD)[35]. This parameter, therefore, can provide information about the transmission of radiation inside a material. The value of OD as a function absorption coefficient (α) and thickness of the sample (d), can be estimated by the relation[35]:

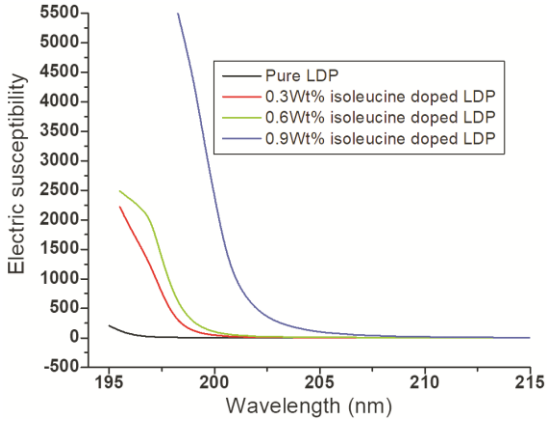


Fig. 10 — A plot of photon wavelength versus electric susceptibility

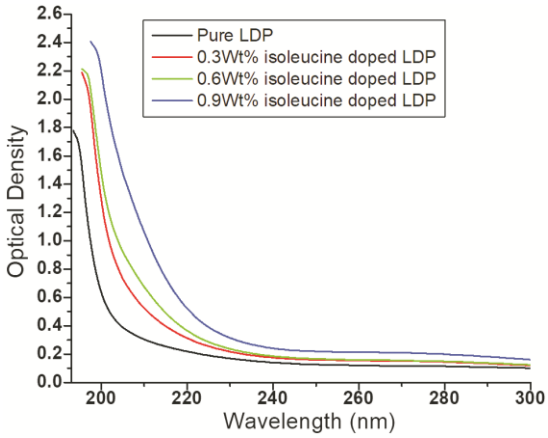


Fig. 11 — A plot of photon wavelength versus optical density

$$OD = 0.434 \times \alpha \times d. \quad \ldots(8)$$

This relation indicates that the value of OD is linearly and directly depends on α and therefore, refractive index n.

Figure 11 shows the curves of OD as a function of wavelength for pure and isoleucine doped LDP crystals. From the Fig. 11, it is observed that all the curves show reduction of OD with increase in wavelength because of reduction of refractive index n with wavelength. The decrease in the value of OD indicates the ability of light to travel through a given medium increases. Further, the value of OD at a constant wavelength is found to increase with increase in doping concentration of isoleucine. It means, the isoleucine doped LDP crystals raises the refractive index of pure LDP crystal and hence, reduces the speed of light passing through the isoleucine doped LDP crystals.

### 3.3 Dielectric Spectroscopic Study

In order to understand the electrical properties and lattice dynamics in the grown crystals of pure and

isoleucine doped LDP, they are subjected to dielectric measurements. For this, the palletized samples were coated with silver paste on opposite surfaces for creating a good conductive layer and then placed between two electrodes. The variation in capacitances (C) and dissipation factor (D) were measured in the frequency range 100 Hz to 1 MHz at room temperature. The dielectric constant (ε') and dielectric loss (ε'') were calculated by the equations:

$$\varepsilon' = C/C_0 = Cd/\varepsilon_0 A \quad \ldots(9)$$

and $$\varepsilon'' = D\varepsilon', \quad \ldots(10)$$

where, d and A are the thickness and cross sectional area of the pellet.

Figures 12 & 13 illustrate ε' and ε'' of pure and isoleucine doped LDP crystals against the frequency of the applied electric field. Both the plots show high value of dielectric constant and loss in the initial range of frequency due to presence of all kinds of polarizations. This is in accordance with the observed

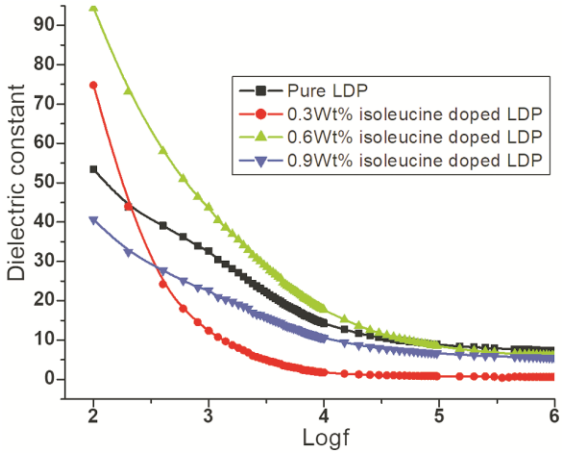


Fig. 12 — A plot of logf versus dielectric constant

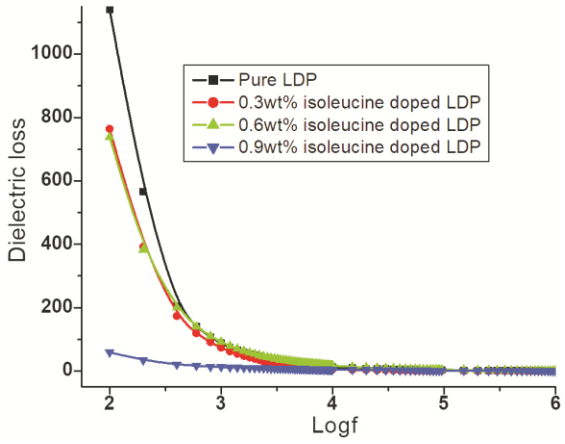


Fig. 13 — A plot of logf versus dielectric loss

variations in dihydrogen phosphate family crystals, *i.e.*, ADP and KDP[36,38]. As the frequency increases, one by one, the contribution of polarization diminishes and at high frequency, because of the inability of the dipoles to follow the applied field, the dielectric constant decreases and becomes independent of frequency of the applied field. This is the normal dielectric behavior of the material[38].

The effect of isoleucine doping and change in its weight% is observed in terms of increase in the value of dielectric constant for 0.3wt% and 0.6wt% isoleucine doped LDP crystals and decrease in the value of dielectric constant for 0.9wt% isoleucine doped LDP crystals. The increased value of dielectric constant for 0.3wt% and 0.6wt% isoleucine doping indicates increase in the effective area of grain to grain contact. This aids in charge transfer and hence results in increase in dielectric constant. For the higher weight% of doping, *i.e.*, 0.9wt%, the effective area of grain to grain contact might be decreased, which hindrances the charge transfer and results in decrease in dielectric constant.

The isoleucine doped LDP crystals show reduced value of dielectric loss. The presence of isoleucine may make the charge carriers inactive. Therefore, it leads to decrease in the conductivity and hence, there is diminution in the value of dielectric loss.

Note that, 0.3wt% and 0.6wt% isoleucine doped LDP crystals possess high value of dielectric constant and low value of dielectric loss compared to pure LDP crystal, which shows that 0.3wt% and 0.6wt% isoleucine doped LDP crystals may be suitable for the application in advanced nanoelectronics for capacity memory devices[39].

#### *3.3.1 AC Conductivity Analysis*

The ac conductivity of pure and isoleucine doped LDP crystals were evaluated by using the equation, which has been used in the literature for the calculation of ac conductivity of ADP and KDP crystals[36,37]:

$$\sigma = \omega\varepsilon_0\varepsilon'', \quad \ldots(11)$$

Figure 14 shows the variation in conductivity as a function of frequency for pure and isoleucine doped LDP crystals. The frequency dependent conductivity curves show a low frequency plateau region and high frequency dispersive region[40,41]. A low frequency plateau region, in which conductivity remains constant and independent of frequency up to certain value of applied frequency, called hopping frequency, can be associated with the dc conductivity of the

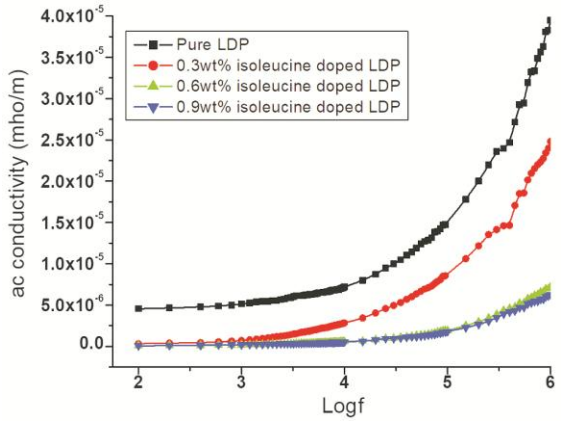


Fig. 14 — A plot of logf versus ac conductivity

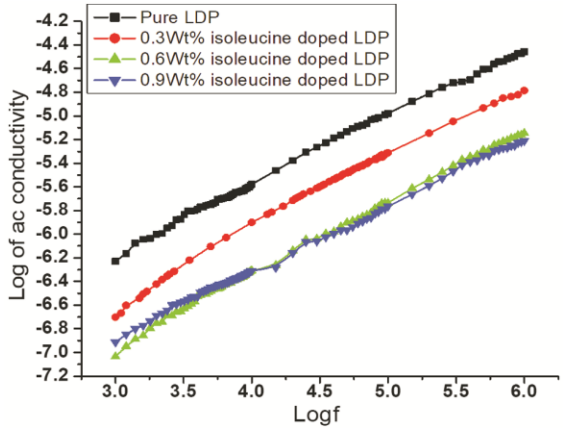


Fig. 15 — Jonscher Plot

Table 3 — Conductivity mechanism related parameters of pure and (0.3, 0.6, 0.9) wt% isoleucine doped LDP crystals

| Sample name | $(\sigma_{dc})10^{-6}$ (S/m) | $(\sigma_{ac})10^{-5}$ (S/m) | s |
|---|---|---|---|
| Pure LDP | 4.54 | 3.94 | 0.59 |
| 0.3wt% isoleucine doped LDP | 0.328 | 2.48 | 0.66 |
| 0.6wt% isoleucine doped LDP | 0.089 | 0.723 | 0.68 |
| 0.9wt% isoleucine doped LDP | 0.085 | 0.625 | 0.68 |

grown crystals[42]. This is the region of frequency in which ions can travel much faster and jump from one site to another available site, the successful jump of which to a neighboring vacant site contributes to the dc conductivity of the sample[42]. From the Fig. 14, it is observed that isoleucine doped LDP crystals show reduced value of dc conductivity, the value of which can be obtained by extrapolating the curves on the y-axis[43] and are listed in the Table 3.

As the frequency exceeds hopping frequency, a high frequency conductivity dispersion region is observed. In this region, the frequency dependence of conductivity can be expressed as[44]:

$$\sigma_{ac}(\omega, T) = A(T)\omega^{s}(T), \quad \ldots(12)$$

where, A(T) is a temperature dependent factor having the unit of conductivity and s is a power law exponent that depends on temperature and composition of the material. This dimensionless parameter generally varies between 0 and 1 and used to characterize the electrical conduction mechanism throughout the sample under investigation[45].

On the log scale, the frequency dependent conductivity can be expressed as

$$log\sigma_{ac} = logA + slog\omega. \quad \ldots(13)$$

From the $log\sigma_{ac}$ versus logf plot, shown in the Fig. 15, called the Jonscher plot, the slope directly provides the value of power law exponent s, which is listed in the Table 3.

From the Table 3, it is observed that the value of s is not zero but s < 1, which indicates that the conduction is frequency dependent or ac conduction[46], which is due to hopping of charges. According to Funke[47], the value of power law exponent has a physical significance based on the value either less than equal to 1 or greater than 1. If power law exponent $s \leq 1$, then the hopping motion of the charge carriers would be a translational motion with a sudden hopping, while for s > 1, the motion of the charge carriers would be a localized motion with a small hopping. Usually, in case of ionic conductors, the value of *n* can lie between 1 and 0.5 indicating the ideal long range pathways and diffusion limited hopping (tortuous pathways)[48]. In the present case, the power law exponent lies between 1 and 0.5 and hence, pure and isoleucine doped LDP crystals possess the above mentioned hopping mechanism of the charge carriers. It is also observed from the Table 3, that s value is found to be high for isoleucine doped LDP crystals. This indicates that a hopping conduction is the predominant mechanism for the samples. The compositional dependence of s can be attributed to the combined effect of distribution of relaxation path, mechanism on the structure like the nature of disorder and the degree of interaction. The higher s value of isoleucine doped LDP crystals could be attributed to the lower rate of successful jumps and in turn result in lower dc conductivity[49] of isoleucine doped LDP crystals.

### 3.4 Impedance Spectroscopy Study

In order to investigate the electrical properties of pure and isoleucine doped LDP crystals, the AC technique of complex impedance spectroscopy is

used. Typical complex impedance plot of pure and isoleucine doped LDP crystals at room temperature along with equivalent electrical circuit model, obtained by using the software Z-view is shown in the Fig. 16.

The curves of each crystal show a trend of bending towards Z' axis and then taking shape of high frequency depressed semicircle, which corresponds to the parallel combination of grain resister ($R_g$) and corresponding capacitor ($C_g$). It would be worth to mention that in the complex impedance plane plot, the formation of full or partial semicircle is affected by the strength of relaxation and the range of frequency used[50,51]. Further, in the low frequency region, no low frequency spikes are observed, which indicates that there is no accumulation of charges at the blocking electrode interface. The presence of single electrical cell describes the electrical properties and the relaxation process of one contribution and in the present case, it is grain contribution. The effect of doping of isoleucine in different wt% is observed in terms of increased diameter of the semicircle. The intercept of the semicircle on real Z' axis gives the value of the grain resistance ($R_g$). It is observed that doping of isoleucine increases the grain resistance of pure LDP crystal. The equivalent circuit parameters are listed in the Table 4.

From the Tables 3 and 4, it can be observed that the increased trend of grain resistance of isoleucine doped LDP crystals is in agreement with the decreased value of dc conductivity of the isoleucine doped LDP crystals. The change in the value of dc conductivity can be explained on the basis of charge carrier density, ion mobility and charge of the ion. The decrease in dc conductivity can be attributed to the decrease in the number of mobile charge carriers and ion mobility due to increased peak width (FWHM) of the isoleucine doped LDP crystals, thereby impeding faster ion transfer process. It is also observed from the Table 4 that, the grain relaxation time is more in isoleucine doped LDP crystals, which indicates that the presence of isoleucine demotes the relaxation process of grain present in the samples.

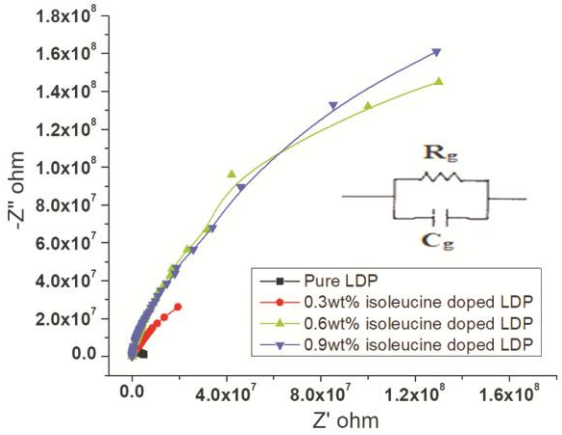


Fig. 16 — Impedance Plot along with equivalent circuit

Table 4 — Equivalent circuit parameters

| Sample | $R_g$ (MΩ) | $C_g$ (pF) | $\tau_g$ (ms) |
|---|---|---|---|
| Pure LDP | 5.37 | 3.68 | 0.0197 |
| 0.3wt% isoleucine doped LDP | 105 | 2.99 | 0.313 |
| 0.6wt% isoleucine doped LDP | 305 | 1.39 | 0.423 |
| 0.9wt% isoleucine doped LDP | 510 | 0.85 | 0.433 |

For the better understanding and to study the effect of isoleucine doping on the relaxation phenomenon, a variation of imaginary part of impedance (Z'') as a function of frequency of pure and isoleucine doped LDP crystals is presented in Fig. 17.

In the inset figure, the same plot for pure LDP and 0.3wt% isoleucine doped LDP crystals is shown because in the combine image, this variation is not seen clearly due to the scaling problem. For pure and 0.3wt% isoleucine doped LDP crystals, the broad and asymmetric relaxation peaks are observed at frequency 2400 Hz and 1600 Hz, respectively. While, 0.6wt% and 0.9wt% isoleucine doped LDP crystals do not show relaxation peaks but a trend of shifting of relaxation peak towards lower frequency side is observed, which may be beyond the lower frequency measurement limit to observe. Hence, doping of isoleucine is observed to shift the relaxation peaks towards lower frequency side compared to pure LDP crystal, indicating increase in the relaxation time and decrease in the rate of successful jump of ions and hence, results into decrease in the value of dc conductivity. The asymmetric peak broadening indicates the distributed relaxation process around the

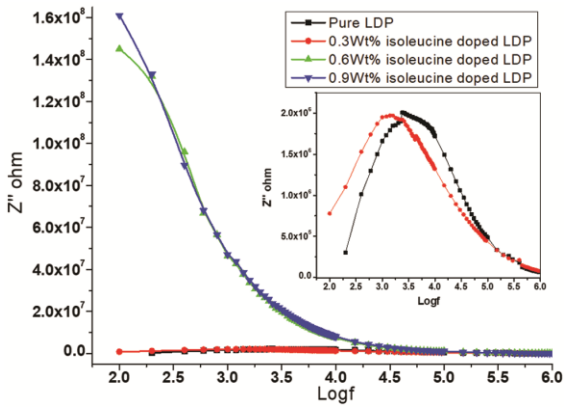


Fig. 17 — A plot of logf versus Z''

mean value and non-Debye type relaxation behavior[52].

The frequency corresponding to $Z''_{max}$ of conductivity relaxation can be correlated with the frequencies corresponding to a change in ion transport from high frequency dispersion region to plateau region in ac conductivity plot, shown in the Fig. 18 for 0.3wt% isoleucine doped LDP crystal.

### 3.5 Modulus spectroscopy study

The modulus formalism is used for the further analysis of impedance data in order to study the conductivity relaxation behavior of pure and isoleucine doped LDP crystals. In terms of complex function, the electric modulus can be written as: $M^* = M' + jM''$, where, M' and M'' are the real and imaginary parts of modulus, respectively[53]. The real and imaginary parts of the complex modulus are evaluated by using the equations given in the literature[54].

Figure 19 shows complex modulus spectrum for pure and isoleucine doped LDP crystals at room temperature, while inset figure shows the same plot

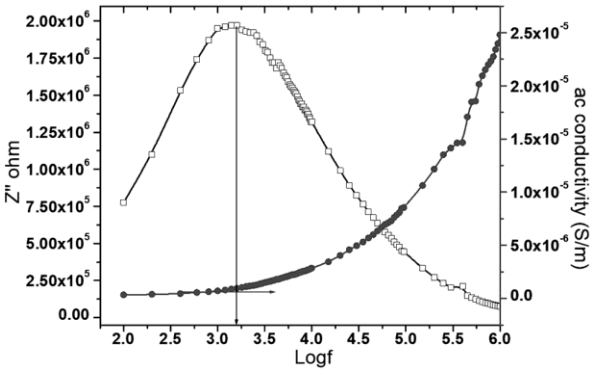


Fig. 18 — Z'' and ac conductivity vs. logf plot for 0.3wt% isoleucine doped LDP crystal

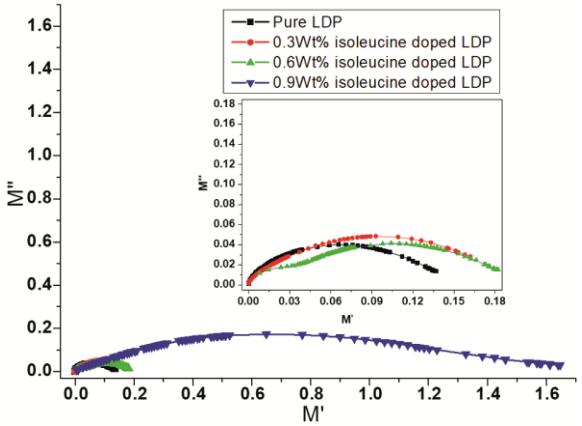


Fig. 19 — Complex Modulus Spectrum

subtracting the data of 0.9wt% isoleucine doped LDP crystal because of its high scale, compared to pure, 0.3wt% and 0.6wt% isoleucine doped LDP crystals.

From the Fig. 19, it is observed that pure and isoleucine doped LDP crystals show arcs in the form of single semi circle, indicating the presence of grain contribution in the grown crystals[50]. None of the curves form complete semicircle as required for the ideal Debye model and the centers of each semicircle appear to lie below the real M' axis, indicating the spread of relaxation with different time constants, hence supports the non Debye type relaxation in the materials[50]. Further, a marked change in the shape and size of the modulus spectrum is observed after isoleucine doping, particularly for 0.9wt% isoleucine doping, which suggests a change in the capacitance value of pure LDP after isoleucine doping. The lowest arc is obtained for the pure LDP crystal, which indicates highest value of grain capacitance of pure LDP crystal, while highest arc is obtained for the 0.9wt% isoleucine doped LDP crystal, which indicates lowest value of grain capacitance of this crystal. The grain capacitance values are listed in the Table 4.

Figure 20 shows the variation of M'' as a function of frequency for pure and isoleucine doped LDP crystals at room temperature. For pure and isoleucine doped LDP crystals, a characteristic peak is observed for a particular value of frequency, where M'' is maximum. The frequency region below M'' maximum is the region in which charge carriers are mobile over long distances and above M'' maximum is the region in which charge carriers are mobile over short distances[53]. Further, the position of the peak of isoleucine doped LDP crystals is observed to change with increase in peak height. For 0.3wt%, 0.6wt% and 0.9wt% isoleucine doped LDP crystals, the peak

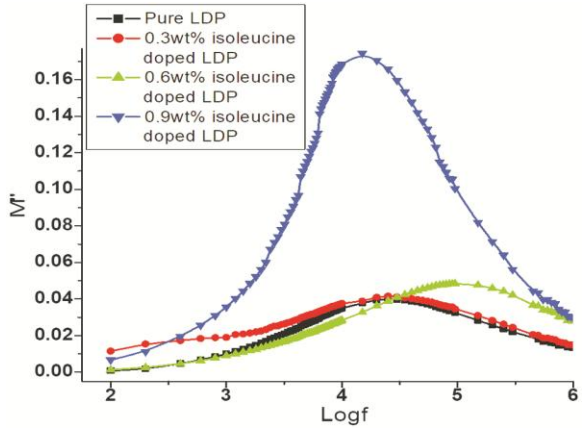


Fig. 20 — A plot of logf versus M''

position is observed at 25000 Hz, 95000 Hz and 15000 Hz, respectively. Such shifting of peak position can be attributed to some variation in microstructure and cation distribution due to the effect of dopant isoleucine on the crystal lattice of pure LDP. Further, the peak height is inversely proportional to the capacitance of the material[55]. Hence, gradual increase in the peak height of isoleucine doped LDP indicates gradual decrease in the value of grain capacitance of isoleucine doped LDP crystals.

Further, the peaks of Z'' and M'' are not observed at the same frequency for pure and 0.3wt% isoleucine doped LDP crystals, i.e., the maxima of Z'' and M'' do not coincide at the same frequency but the peak of Z'' is observed at lower frequency, whereas the peak of M'' is observed at high frequency for pure and 0.3wt% isoleucine doped LDP crystals. Elaborately, for pure LDP crystal, Z'' and M'' peaks are observed at 2400 Hz and 25000 Hz, respectively, while the same are observed for 0.3wt% isoleucine doped LDP crystal at 1600 Hz and 25000 Hz, respectively. This indicates that the first condition of ideal Debye type dielectric relaxation, i.e., the impedance ($Z^*$) and the modulus ($M^*$) maxima peaks should occur at the same frequency, is not satisfied and hence, resulting into the existence of non-Debye type relaxation mechanism in the grown crystals of pure and isoleucine doped LDP[56,57].

#### *3.5.1 Scaling behavior of M''*

In order to carry out the scaling behavior of M'' at room temperature for the pure and isoleucine doped LDP crystals, the $M''_{max}$ and $f_{max}$ are used as the scaling parameters for M'' and f, respectively. The scaled imaginary part of modulus at room temperature for pure and isoleucine doped LDP crystals are shown in the Fig. 21.

The scaling behavior is used to determine the temperature dependent or temperature independent dynamic process occurring within samples for the study which is carried out by varying the temperature of the samples or it is used to determine the dopant dependent or dopant independent dynamic process occurring within samples for the study which is carried out by varying the concentration of the dopant. In the literature[36], report is available on such type of study. It can be seen from the Fig. 21 that, the scaled spectrum of modulus remains distinguishable, hence indicates that the relaxation dynamics of charge carriers occurring within the grown crystals do not follow a common mechanism but vary as per the concentration of the charge carriers, which may vary as per the wt% of the dopant isoleucine. This indicates the dopant and its weight % dependent nature of the ion conductivity mechanism.

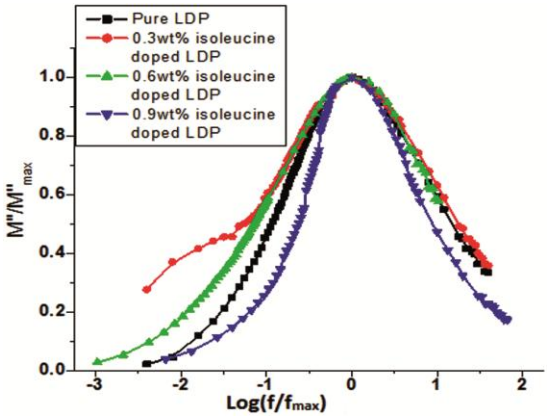


Fig. 21 — Scaled modulus spectra

Table 5 — Exponent parameter (β) values

| Sample name | β value |
|---|---|
| Pure LDP | 0.61 |
| 0.3wt% isoleucine doped LDP | 0.70 |
| 0.6wt% isoleucine doped LDP | 0.75 |
| 0.9wt% isoleucine doped LDP | 0.95 |

In order to investigate whether the dynamic relaxation process present within pure and isoleucine doped LDP crystals is ideal De-bye type or not, the stretch exponent parameter is evaluated by using the formula[58,59]:

$$\beta = \frac{1.14}{FWHM} \quad , \qquad ...(14)$$

Here, FWHM is the full width at half maximum of M'' versus logf curve obtained from its Gaussian type curve fitting. The obtained values are summarized in the Table 5.

From the Table 5, it is observed that the lowest value of β is obtained for the pure crystal of LDP, which indicates a greater departure from the ideal Debye response. As isoleucine is doped and as its weight % increases gradually, the β value approaches to 1, which shows that the effect of isoleucine improves the relaxation behavior of the pure LDP crystal. This also becomes clear from the curves of scaled behavior of modulus as well as from the spectroscopic curve of modulus, *i.e.*, M'' versus logf curve.

## 4 Conclusion

The pure and isoleucine doped LDP crystals were grown by slow solvent evaporation technique. Powder XRD analysis suggested that all the grown crystals

possessed single phase nature and belonged to orthorhombic crystal system. The doping of isoleucine resulted into decrease in crystallite size and increase in FWHM of the most intense peak. W-H analysis showed the presence of both compressive and tensile strain in the grown crystals. The doping of isoleucine showed reduction in the bandgap value. The Urbach tail of the absorption edge shifted towards lower energy side with increase in doping concentration of isoleucine and inverse relationship was found between bandgap energy and Urbach energy. The extinction coefficient exhibited very low and saturated value within medium and large wavelength uv region and visible region. The doping of isoleucine increased the extinction coefficient value. The magnitude of skin depth decreased gradually with increase in doping concentration of isoleucine. The refractive index showed normal dispersion behavior and increased progressively on increasing the isoleucine doping concentration. The isoleucine doped LDP crystals showed higher optical conductivity than pure LDP crystal with shifting of plateau towards lower photon energy. The isoleucine doped LDP crystals showed very high value of susceptibility compared to pure LDP crystal, revealed a significant response of isoleucine doped LDP crystals to be polarized in the applied electric field. Optical density was found to increase on isoleucine doping. Dielectric constant and loss showed normal dielectric behavior. A decrement in the conductivity was observed on isoleucine doping. The power law exponent indicated the ideal long range pathways and diffusion limited hopping mechanism of the charge carriers and supported the conductivity results. The complex impedance and modulus plot analysis confirmed the grain contribution in the relaxation process. The effect of isoleucine doping was observed in terms of increase and decrease in the grain resistance and capacitance, respectively. The different peak positions of Z'' and M'' spectra confirmed the distributed relaxation time and non De-bye nature of relaxation. The lowest value of β of pure LDP crystal indicated greater departure from ideal De-bye type behavior. The doping of isoleucine was observed in terms of improved relaxation behavior. The scaling behavior showed the dopant and its weight % dependent nature of the ion conductivity mechanism.

## Future Direction

Lithium dihydrogen phosphate (LDP) materials may focus on enhancing battery performance, advancing optical device technologies, exploring biomedical applications, and developing energy harvesting and environmental remediation solutions. LDP materials offer advantages such as high dielectric constant, piezoelectric properties, optical transparency, and biocompatibility, making them promising candidates for a wide range of applications in batteries, optics, and beyond. Continued investigation into LDP materials is expected to drive innovation and contribute to advancements in energy storage, photonics, biomedicine, and environmental engineering.

## Acknowledgements

The authors are thankful to HOD, Physics, Saurashtra University, Rajkot for their keen interest and support for dielectric data measurement. Author (H. K. Ladani) thankful to Laxmi Hathiya for help in dielectric data collection.

## References

1 Susic M V & Minic D M, *Solid State Ionics*, 2 (1981) 309.
2 Lee K S, Moon J, Lee J & Jeon M, *Solid State Commun*, 147 (2008) 74.
3 Haussuhl S, *Cryst Res Technol*, 31 (1996) 323.
4 Baranov A I, *Crystallogr Rep*, 48 (2003) 1012.
5 Iurchenka A N, Voronov A P, *et al*., *Functional Materials*, 21 (2014) 324.
6 Rhimi T, Leroy G, Duponche B, Khirouni K, Guermazi S, Toumi M, *Ionics*, 24 (2018) 1305.
7 Kweon J J, Fu R, Steven E, Lee C E & Dalal N S, *J Phys Chem C*, 118 (2014) 13387.
8 Catti M & Ivaldi G, *Zeitschrift für Kristallographie*, 146 (1977) 215.
9 Haussu S, *Cryst Res Technol*, 3 **(**1996) 323.
10 Catti M & Ivaldi G, *Z Kristallogr*, 146 (1977) 215.
11 Lee K S, Oh I H, Kweon J J, Lee C E & Ahn S H, *Mater Chem Phys*, 136 (2012) 802.
12 Soboleva L V & Smolsky I L, *Crystallogr Rep*, 42 (1997) 700.
13 Voronov A P, Babenko G N, Puzikov V M Iurchenko & A N, *J Cryst Growth*, 374 (2013) 49.
14 Hasmuddin M, Singh P, Shakir M, Abdullah M M, Vijayan N, Ganesh V & Wahab M A, *Mater Chem Phys*, 144 (2014) 293.
15 Joshi J H, Joshi G M, Joshi M J, Jethva H O & Parikh K D, New J Chem, 42 (2018) 17227.
16 Iurchenko A N, Voronov A P, Roshal A D, Kryvonogov S I, Babenko G N & Pritula I M, *Funct Mater*, 24 (2017) 226.
17 Catti M & Ivaldi G, *Zeitschrift fur Kristallographie*, 146 (1977) 215.
18 Nasiri–Tabrizi B, *J Adv Ceram*, 3 (2014) 31.
19 Balboul M R, Schock H W, Fayak S A, Abdel El-Aal A, Warner J H & Ramadan A A, *Appl Phys A Mater Sci Process*, 92 (2008) 557.
20 Williamson G K & Hall W H, *Acta Metal*, 1 (1958) 22.
21 Jayasankar K, Pandey A, Mishra B K & Das S, *Mater Chem Phys*, 171 (2016) 195.

22 Ahlawat A, Sathe V G, Reddy V R & Gupta A, *J Magn Magn Mater*, 323 (2011) 2049.
23 Solanki P, Oza M, Jethva H, Joshi G & Joshi M, *Mater Today Proc*, 67 (2022) 879.
24 Paul T C & Podder J, *Appl Phys A*, 125 (2019) 818.
25 He T, Ehrhart P & Meuffels P, *J Appl Phys*, 79 (1996) 3219.
26 Joshi J H, Dixit K P, Parikh K D, Jethva H O, Kanchan D K, Kalainathan S & Joshi M J, *J Mater Sci Mater Electron*, 29 (2018) 5837.
27 Suriya M, Manimaran M, Boaz B M & Murugesan K S, *J Mater Sci Mater Electron*, 32 (2021) 11393.
28 Urbach F, *Phys Rev*, 92 (1953) 1324.
29 Zahan M & Podder J, *J Mater Sci Mater Electron*, 30 (2019) 4259.
30 Bakr N A, Funde A M, Waman V S, Kamble M M, Hawaldar R R, Amalnerkar D P, Gosavi S W & Jadkar S R, *J Appl Phys*, 6 (2011) 519.
31 Pankov J I, Optical processes in semiconductors, Dover, New york, (1975) 428.
32 Yakuphanoglu F, Cukurovali A & Yilmaz I, *Opt Mater*, 27 (2005) 1363.
33 Jayaprakash P, Mohamed M P & Caroline M L, *J Mol Struct*, 1134 (2017) 67.
34 Patterson J D & Bailey B C, Solid-State Physics-Introduction to the Theory, Springer, 3rd Edn, (2018) 649, https://doi.org/10.1007/978-3-319-75322-5.
35 Abd-Elnaiem A M, Abdelraheem A M, Abdel-Rahim M A & Moustafa S, *J Inorg Organomet Polym Mater*, 32 (2022) 2009.
36 Vadhel K V, Joshi J H, Kochuparampil A P, Kalainathan S, Joshi M J & Jethva H O, *Opt Mater*, 134 (2022) 113136.
37 Bhuva H, Vadhel K V, Joshi M J & Jethva H O, *Int J Sci Res Phys Appl Sci*, 10 (2022).
38 Anderson J C, Dielectrics, Chapman and Hall, London, (1964) 16.
39 Lu J, Moon K S, Xu J & Wong C P, *J Mater Chem*, 16 (2006) 1543.
40 Osman Z, Ghazali M, Othman L & Isa K, *Result Phys*, 2 (2012) 1.
41 Shukla N, Thakur A K & Marks A S D T, *Int J Electrochem Sci*, 9 (2014) 7644.
42 Gohel K & Kanchan D K, *J Adv Dielect*, 8 (2018) 1850005.
43 Lee W K, Lim B S, Liu J F & Nowick A S, *Solid State Ionics*, 53 (1992) 831.
44 Bhat B H, Samad R & Want B, *Appl Phys A*, 122 (2016) 1.
45 Issaoui H, Benali A, Issaoui F, Dhahri E, Costa B F O, Graca M P F, Valente M A & Lamjed M, *RSC Adv*, 11 (2021) 33070.
46 Batoo K M, *Phys B*, 406 (2011) 382.
47 Funke K, *Prog Solid State Chem*, 22 (1993) 111.
48 Mauritz K A, *Macromolecules*, 22 (1989) 4483.
49 Elliott S R & Owens A P, *Philos Magn*, 60 (1989) 777.
50 Ranjan R, Kumar N, Behera B & Choudhary RNP, *Adv Mat Lett*, 5 (2014) 138.
51 Garhardt R J, *Phys Chem Sol*, 55 (1994) 1491.
52 Sen S & Choudhary R N P, *Mater Chem Phys*, 87 (2004) 256.
53 Sharma P, Kanchan D K, Gondaliya N, Paunt M & Jayswal M S, *Ionics*, 19 (2013) 301.
54 Joshi J H, Kanchan D K, Jethva H O, Joshi M J & Parikh K D, *Ionics*, 24 (2018) 1995.
55 Thansanga L, Shukla A, Kumar N & Choudhary R N P, *Phase Trans*, 94 (2021) 47.
56 Prabakar K, Narayandass S A K & Mangalaraj D, *Cryst Res Technol*, 37 (2002) 1094.
57 James A R, Prakash C & Prasad G, *J Phys D: Appl Phys*, 39 (2006) 1635.
58 Aziz S B, Abidin Z H Z & Arof A K, *Exp Polym Lett*, 4 (2010) 300.
59 Jonge J J de, Zon A V, Leeuw S W de, *Solid State Ionics*, 147 (2002) 349.